Mechanical response of soil mixtures under Freezing and Thawing processes

Bachelor Thesis Report

UNIVERSITY OF TWENTE.

Author: Nicolás González Pérez

Supervisors: dr. ir. Floriana Anselmucci, Giulia Guida

Second Assessor: Philippe Frankemölle

Date: 9th of July 2024

Student Number: 2690969

Study: Bachelor Civil Engineering

Version: Final version

1. Abstract

This study investigated the mechanical response of soil mixtures subjected to freezing and thawing cycles (abbreviated to FT cycles in this report). The research focused on understanding how these cycles affect the shear strength characteristics of various soil mixtures, which is especially crucial for construction in cold regions where cyclical freezing and thawing of the ground occurs multiple times throughout the year.

The study consisted of conducting the direct shear test on mixtures of sand and clay. Initially six mixtures of differing proportions of sand and clay were prepared, but two were soon discarded. Per mixture three batches of three samples each were tested, so nine samples per mixture in total. The batches pertained to the state of the samples when being tested: dry, saturated, and subjected to FT cycles. The tests measured the shear force, vertical displacement, and horizontal displacement under an imposed normal stress. This normal stress was predetermined and differed per sample in a batch of a mixture, so that each batch consisted of identical samples each tested with a different normal stress. From the experiment measurements, parameters such as void ratios, volume deformation, shear stress, cohesion and friction angle were derived and analysed.

The findings indicated that soil mixtures with a fine content of 20% or above demonstrated an erratic mechanical response under FT cycles, but also when saturated or when dry. It was seen that for these mixtures the shear strength decreased for increasing normal stress and showed no difference between dry, saturated and FT states, which opposed the main hypotheses drawn from the literature. An important finding was that these mixtures often had excessive contraction which rendered them unfit for shear testing. In the case of the mixtures with a fine content below 20%, the shear strength generally increases with higher normal load. These mixtures showed more predictable behaviour, with clear trends in shear strength and volume deformation. However, the strength of the dry samples was not always greater than that of the FT samples, another main hypothesis of the literature. This led to the conclusion that a higher degree of FT cycling is necessary to observe more pronounced results, meaning lower freezing temperatures and more cycle iterations.

The study concluded that FT cycles can significantly impact the mechanical properties of soil mixtures, but a higher degree is needed to fully visualize this impact. Further research is recommended especially in terms of the high fine content mixtures to investigate the erratic behaviour shown in this study and justify it. Additional further testing could also incorporate refinements to the methodology, particularly in the preparation of samples, the measurement of important parameters such as the void ratio, and considerations of more intense FT cycling.

Table of Contents

2. Introduction

The study of soil mechanics for engineering and construction is vital to ensure infrastructure is properly built and remains stable. Soil is a multiphase medium, meaning a medium containing substances of multiple different states of matter (Kadivar & Manahiloh, 2019). This results in complex mechanical properties that do not follow the usual patterns of single-phase media. One of the main properties of soil that greatly impacts its behaviour is water content. Soil is a porous medium, so it has a high water absorption and retention ability. Depending on the water content of a soil sample, its mechanical properties vary. In very cold regions of the world, soils experience Freezing and Thawing cycles throughout the year. This raises questions about the effects of these cycles on soil and the subsequent implications in construction on these soils.

The phase change of the pore water from liquid into solid ice due to freezing temperatures significantly improves the overall hydro-mechanical behaviour of the soil, making it stronger, stiffer and impervious. However, the microstructure change induced by the volume expansion upon freezing and the severe contraction of ice-rich soils during thawing significantly degrade the material, leading to critical issues for the stability and functionality of the neighbour structures.

Still, however, our current understanding of the inherent change mechanism in the mechanical behaviour of frozen soil is incomplete and related reports are rare. Hence, it requires further investigation, especially when the water content changes in the saturation scale, causing further changes in density, liquid limits and related mechanical parameters (Sun et al., 2022).

This report details a study on the mechanical response of soils that have undergone Freezing and Thawing cycles. The study will be of experimental nature, consisting of the performance of a direct shear test on samples that have undergone induced Freezing and Thawing cycling as well as saturated and dry samples to draw comparisons.

The structure of this document is as follows. Firstly, the project is introduced, detailing the background and scope of the problem, the research motivation, problem statement, research questions and methodology. Then, the experiment preparation and execution are described, followed by the experiment results. Finally, a discussion on the results reflects on the experimental process and a conclusion follows summarizing the findings.

2.1 Problem Context

Frozen soils are considered a 4-phase medium (Kadivar & Manahiloh, 2019), consisting of a mixture of mineral and sometimes organic solid soil particles, ice, water and gases of different compositions (Sun et al., 2022). Figure 1 shows a diagram of a microscopic view of frozen soil particles.

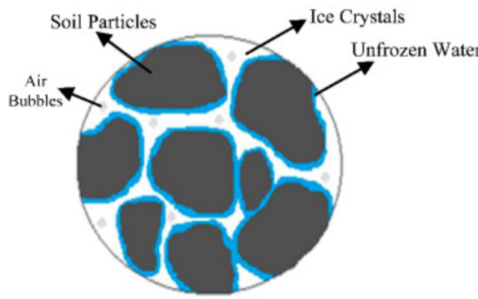

Figure 1:Diagram of microscopic view of frozen soil particles (Kadivar & Manahiloh, 2019)

Therefore, frozen soils contain 2 solid phases, the soil particles and the ice crystals, unlike saturated or unsaturated soils (Kadivar & Manahiloh, 2019). The latter two pertain to the soil sample's water content, wherein saturated soil indicates that all the pores are filled with water and the soil has absorbed as much water as it can hold, with the soil surface being below the water table level (Plantiago.com, 2023).

Due to the presence of two solid phases in frozen soils, the effective stress as a component of the total stress differs from the Terzaghi standard for saturated soils. The effective stresses of unfrozen unsaturated soils, in which voids are filled by water and air, are typically expressed by the following equation (Kadivar & Manahiloh, 2019):

$$\sigma'_{ij} = (\sigma_{ij} - P^a\delta_{ij}) + \chi \, P_c\delta_{ij} \qquad \text{(Equation 1)}$$

Where, σ'_{ij}= the effective stress, σ_{ij}= the total stress, P^a= the air pore pressure, χ= the effective stress parameter, P_c= the capillary pressure/matric suction, δ_{ij}= the unit tensor.

In simpler terms, the equation above shows how the effective stress depends on the total stress and on the water and air pressures.

When temperatures fall below 0ºC, the pore water in the soil freezes and the joint presence of water and ice induces a negative pore pressure. This is due to the differences in water and ice pressures (different densities and specific weights thus different pressures) that is known as cryogenic suction (Kadivar & Manahiloh, 2019). At the interface between water and ice, a cryogenic suction gradient develops, which causes erosion known as ice segregation. Water migration, a movement of water from unfrozen to frozen soil occurs, lowering the water content and pore pressure of the unfrozen section and thus increasing consolidation.

Furthermore, water accumulation and the volumetric expansion of water as it turns into ice lead to frost heaving (Xu et al., 2020), the upward or outward expansion of a soil surface attributed to the development of ice within the soil layer (Murton, 2021). Heaving takes place in the direction of least resistance and perpendicular to the ice layer, and therefore usually upwards. This results in soil that is stronger, stiffer and more impermeable. Figure 2 shows a visual representation of the freezing process of soil and the changes induced in the temperature, pore pressure and displacement profiles.

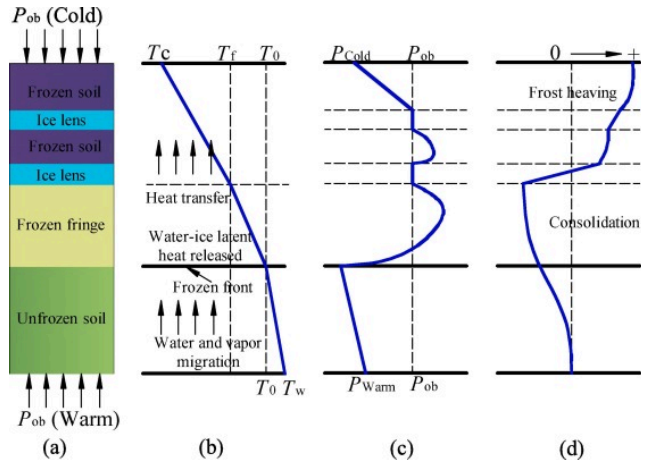

Figure 2: Visual representation of changes in physical properties of soil due to freezing. (a) depicts soil layers at different freezing states, with P_{ob} representing the surface overburden stress. (b) shows the temperature gradient change. (c) denotes the pore pressure profile. (d) depicts the displacement profile, showing the 0 displacement line and how frost heaving occurs at frozen soil, and consolidation occurs at the frozen fringe (Xu et al., 2020).

Naturally, and as described by Figure 2, these physical changes are reversed when soil thaws. As shown by the displacement profile, the soil layer can return to the 'initial' state or position, which supposes an expansion of the consolidated region, lowering its strength, and compression of the frost-heaved layer of the soil causing a reduction of the shear strength. This compromises the stability and functionality of infrastructure built on the soil and causes foundational distress. This distress ranges from longitudinal cracks at the embankment surface to lateral spreading or tilting of the side slopes (De Guzman et al., 2018).

These effects are exacerbated when the soil is subjected to a Freezing and Thawing cycle (FT cycle in short). This cycle triggers physical effects that can cause significant structural changes to soil (Tang et al., 2018). This can be used advantageously, for example, Artificial Ground Freezing is an earth-supporting technique for excavations that helps prevent contour instabilities and water inflow. Still, in many regions challenges persist including anomalous movements caused in road pavements due to soil heaving, railroad distortion or slope sliding (Shastri et al., 2021).

For example, in Hokkaido, Japan, up to 25% of slopes used for built-up areas experienced failure during the thawing season. A study conducted in the area discovered that the soil shear strength decreased when the temperature exceeded the freezing point of water, 0ºC (Kadivar & Manahiloh, 2019). Therefore, the shear strength is very important in ensuring the long-term stability of infrastructure built on soil subjected to FT cycling (De Guzman et al., 2018). Shear strength is defined as the maximum resistance the soil can oppose to shearing movements (Hossain et al., 2021a).

Shear failure is commonly characterised by sliding of the soil plane. General shear failure is characterised by tilting due to constant bulging of the soil, as a result of a failure surface developing between the edge of the footing and the ground surface. Local shear failure is observed in loose or weak soil, because of notable compression of the soil and a partial plastic equilibrium. Punching shear failure occurs due to a large soil settlement (Mishra, 2017).

Due to the continuously developing effects of climate change and soil degradation by human activities, the consequences of soil mechanical response under FT cycles on the infrastructure are progressively more common and higher in magnitude (Sun et al., 2022). Still, studies on this occurrence are sparse, especially in terms of water content and soil fine content. The mechanical response constitutes the stress-strain relationship. In particular, the stress-strain relation. It was hypothesised that the samples subjected to FT cycling would present a lower shear strength as per the literature discussed above.

2.2 Problem Statement

The reasoning behind this study is the investigation of the phenomena related to FT cycling of soil mixtures, particularly in terms of material and strength degradation, and how due to climate change and human-driven soil deprivation, this is expected to worsen over time. However, studies are rare and conclusions are sparse, so it is highly uncertain to which extent these phenomena pose a threat to modern infrastructure and construction projects. Therefore, this study investigated saturated samples under induced FT cycling using direct shear testing and compared them with saturated and dry samples at room temperature. This made it possible to draw a relation between the shear strength and the strain of the soil and assess how this relation is affected by the FT cycling.

2.3 Research Dimensions

2.3.1 Research Aim

The proposed experimental study aimed to investigate the response of saturated soil samples under induced Freezing and Thawing cycles. The aim was to gain a better understanding of the evolution of soil mechanical properties under controlled freezing and thawing patterns, and how it contributed to explaining and predicting the complex phenomena related to freezing of soil as discussed in Tang et al. (2018) and Xu et al. (2020), to be able to prevent possible negative effects of these phenomena.

In particular, it investigated how the initial properties of a soil sample impacted the mechanical response, such as density and fine content, so as to predict which initial conditions of the soil might become problematic after inducing an FT cycle. The experiment was conducted on dry and saturated samples to draw comparisons. The initial properties of a saturated soil sample are a degree of saturation of 100%, high compressibility due to the lack of air voids, reduced shear strength (increased water content reduces friction between particles and enhances sliding), high permeability due to water-filled voids, elevated pore pressure and swelling (Yin et al., 2020). Only some of these properties can be controlled and imposed in the experiment, namely the degree of saturation and the sample density, which can be loose if the initial void ratio is close to the maximum void ratio, or dense if the initial void ratio is close to the minimum one.

This research was practice-oriented, based on conducting a soil direct shear test using three different batches of samples, dry, saturated and subjected to FT cycling (referred to as FT).

2.3.2. Research Questions

From the problem context and research aim, research questions can be derived to drive the analysis and realise the research aim. The main research question is:

How does the shear strength of the soil mixtures change when it is subjected to Freezing and Thawing cycles?

This question covers the research scope as established in Section 2.1, *Problem Context*, in the broadest sense. Further subquestions were developed regarding the experimental process and research aim.

1. *Which initial conditions impact the mechanical response of the soil mixture the most?*
   a. *What is the impact of the initial soil density?*
   b. *What is the impact of the soil fine content?*
2. *How does the FT cycling affect the shear strength?*
   a. *What is the difference in shear response between a sample subjected to FT cycling and a sample not subjected to FT cycling?*
3. *How can the results be interpreted?*
   a. *To what extent does the Mohr-Coulomb criterion depict the decrease in strength properties of the soil due to FT cycling?*
   b. *Which aspects of the methodology affect the uncertainty in the results?*

2.4 Research Methodology

This section outlines the method and process used to conduct the analysis. The research was practice-oriented, therefore it was based on an experimental approach. This consisted of the soil direct shear test, and was conducted alongside the Soil Micro Mechanics Chair at the University of Twente.

The experiment was conducted for various mixtures of sand and clay, for which there were three batches: FT samples (subjected to FT cycling), Saturated samples and Dry samples. Ideally, the experiment can be conducted on soil samples collected directly from the field. However, the collection of frozen undisturbed samples is costly and challenging. Furthermore, the undisturbed samples might have a range of water contents, densities and soil types, whereas this experiment is designed for saturated samples. Therefore, reconstituted saturated samples were used to ensure the water content remained constant (Shastri et al., 2021).

Hence, artificial mixtures of sand and clay already gathered at the lab were employed. The initial features of these samples will be measured, such as fine content, and some initial conditions for the samples were established that must hold for all samples used in the experiment to ensure consistency. Some of these conditions included the height, area, volume, diameter and specific gravity of the soils, and some calibration factors of the apparatus.

The sample preparation can be organised as follows:

1. Dry mixing together a given proportion of sand and clay.
2. Spooning the soil into the shear box sample and compacting it according to the desired density state.
3. Measuring the dry initial state of the sample, so the volume, mass and void ratio.
4. Saturating the mixture.
5. Measuring the wet initial state of the sample.
6. Imposing the desired degree of FT cycling.

Figure 3 illustrates a scheme of the shear test apparatus. The direct shear test consists of applying a normal load first and then horizontally displacing the top half relative to the bottom half to induce shear deformation and measure the shear stress.

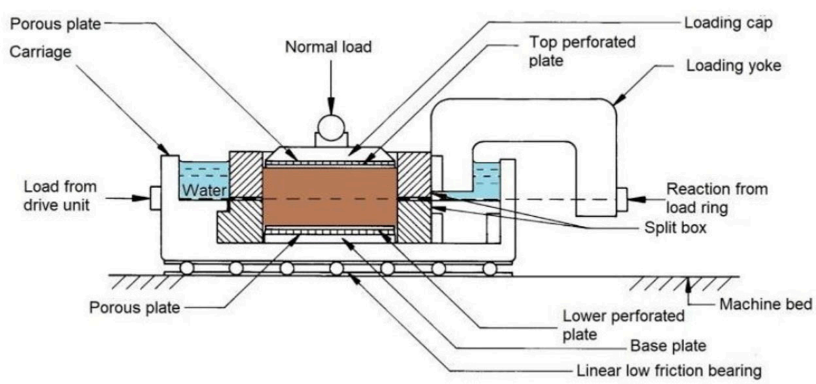

Figure 3: Diagram of direct shear test experiment system setup (Brian, 2019).

The device contains three measurement sensors: a vertical displacement transducer, a horizontal displacement transducer and a shear load cell. These measure the vertical displacement, horizontal displacement and shear force respectively. The vertical load is set to a predetermined initial value. Readings are taken until after the horizontal shear stress reaches a peak value and converges at a residual value, or until the horizontal displacement reaches an imposed value (Hossain et al., 2021a). Therefore, the raw data consists of the following quantities:

- Vertical displacement (in mm)
- Horizontal displacement (in mm)
- Shear force (in N)

From these, the shear stress was derived, dividing by the area of the shear box. The most optimal way of displaying this data is by making plots, for example: a horizontal displacement and stress plot, a volume change and horizontal displacement plot, and a normal stress and peak shear stress plot. Examples of these are shown in Figures 4, 5 and 6.

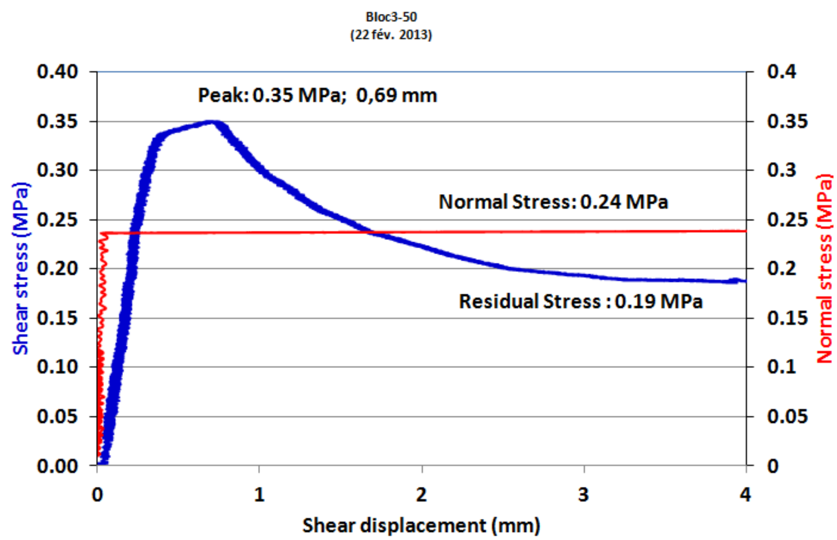

Figure 4: Relation between the shear stress and the horizontal (shear) displacement (Moradian et al., 2013)

Figure 4 shows the evolution of the shear stress (blue curve) and the normal stress (red curve) at increasing shear displacement. It can be seen that the shear stress reaches a peak and declines after that. The aim of the experiment was to retrieve this peak of shear stress, considered to be related to the shear strength of the sample. It can also be seen that the normal stress increases until it becomes constant because, unlike the shear stress, it is imposed by the experiment and therefore does not vary. It is also important to examine the deformation of the volume of a sample as it undergoes shearing, particularly to determine the density state of the soil so as to understand if the soil contracts or dilates.

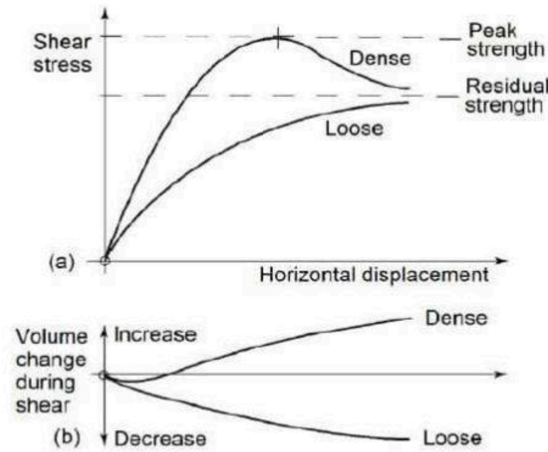

Figure 5: Soil density state depending on shear stress and volume deformation (Head & Epps, 2011).

Figure 5 shows how the shape of the curves can denote the density state of the soil during the shearing stage. It is expected that the soil presents a dense state and dilates if it previously compacted in the preparation of the sample. Since the soil is subjected to a combination of normal and shear stresses and the normal stress is imposed and constant, it can be plotted against the peak shear stress (also known as the shear strength).

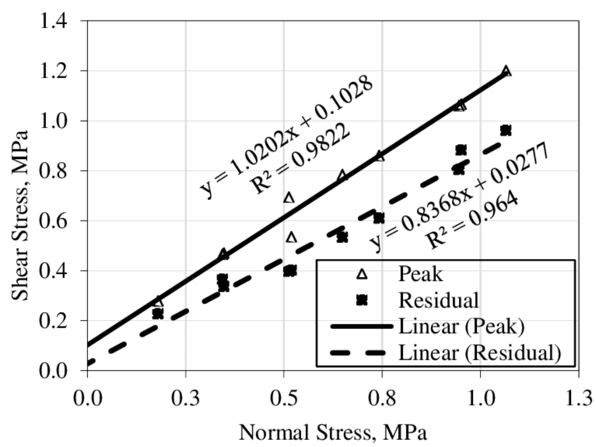

Figure 6: Shear stress vs normal stress plot (Dev et al., 2018)

Figure 6 shows a shear stress against normal stress plot, also known as a Failure Envelope. This plot consists of the imposed normal stress and the peak shear stress of each test, to show the combination of stress values at which the soil sample experiences failure. Here, the normal stress is the independent variable. The goal is for the points, representing the experimental data, to lie in a linear locus corresponding to the Mohr Coulomb criterion, shown in Equation 2.

$$\tau = c' + \boldsymbol{\sigma} \tan(\boldsymbol{\phi}) \qquad \text{(Equation 2)}$$

Where, τ = shear stress, $\boldsymbol{\sigma}$= normal stress, c'= effective cohesion, $\boldsymbol{\phi}$= friction angle

By fitting the experimental data with Equation 2, the effective cohesion and friction angle of the material can be deduced. The cohesion is the internal strength or bonding between soil particles that enables the soil to resist shear forces; it can also be described as the non-frictional shear resistance (Prasad, 2023). The friction angle describes the frictional shear resistance of the soil relative to the normal effective stress (User, 2013). As a multiphase medium, soil does not just fail due to a particular value of normal or shear stress, but due to a combination of both. The most common method of measuring stress changes at different loading stages is using the Mohr's Circle diagram (see Figure 7). Mohr's Circle is a graphical representation of soil stress distribution, where each point in the circle represents a certain plane which has corresponding values of normal and shear stress (Pratik, 2023).

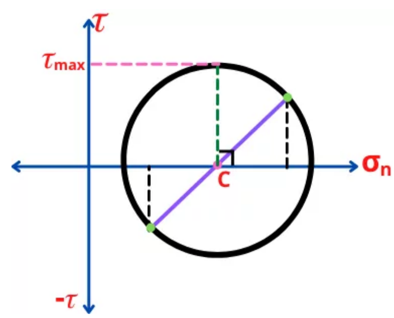

Figure 7: Mohr's Circle diagram. $\boldsymbol{\sigma}_n$ Represents the maximum normal stress and τ_{max} the maximum shear stress (Pratik, 2023).

Mohr's circle can be drawn for a soil sample and alongside the failure envelope. Any points where these two intersect correspond to a combination of stresses that causes failure. This is difficult to visualise if multiple circles have to be drawn on the same plane, due to little correlation between observations. Therefore, a stress path is optimal to easily represent the changes in stress. A stress path is a linear or curve-shaped locus of several points that represents the changes in stress of a soil sample (Obinna, 2021). The goal is for the points to lie in a linear locus, as shown in Figure 8.

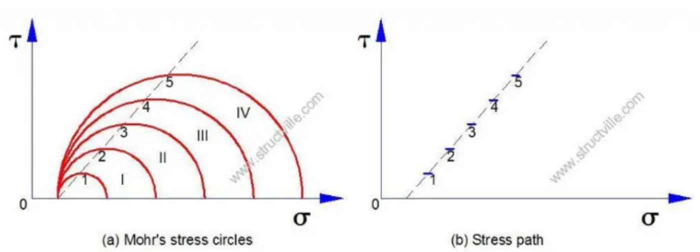

Figure 8: stress path (Obinna, 2021)

Each value of the stress path is λ times the previous value, where λ is an eigenvalue. The coordinates of a point in the stress path are given by the following equation:

$$(\boldsymbol{\sigma}_1 + \boldsymbol{\sigma}_3)/2 \text{ and } (\boldsymbol{\sigma}_1 - \boldsymbol{\sigma}_3)/2 \qquad \text{(Equation 3)}$$

To obtain a linear locus, the same mixture must be tested at least three times with different normal stresses. Thus, the stress path should have at least 3 points and each normal stress applied should be an eigenvalue of the previous test.

The full research process is schematised in the research model shown below. This is an overview of how the research questions relate to the steps of the experimental process, and ultimately lead to the research aim.

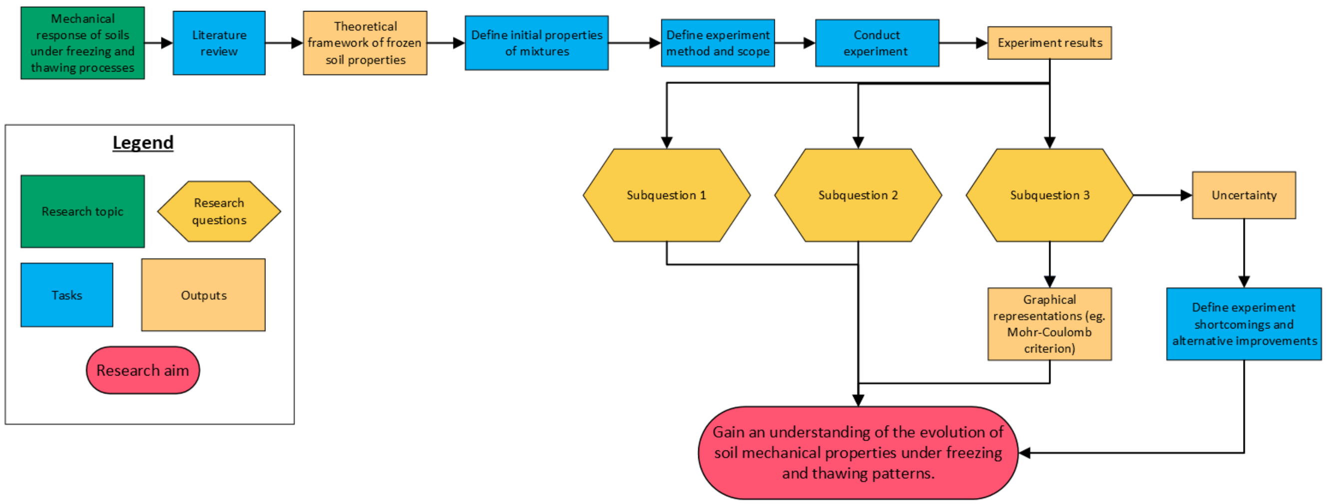

Figure 9: research model

3. Experiment preparation & execution

The first step as given by Figure 9 is to define the characteristics of the mixtures. This starts with the sample preparation, for which the steps are laid out in Section 2.4 *Research Methodology*. For this experiment, two types of soil will be used. The first is kaolin Speswhite, a fine, white clay that will be the fine content of the mixtures. The second is sand, already gathered at the lab, which was sieved to obtain a grain size distribution similar to that of Fontainebleau Sand. Table 1 shows the grain size distribution of 1kg of the sand mixture.

Table 1: grain size distribution

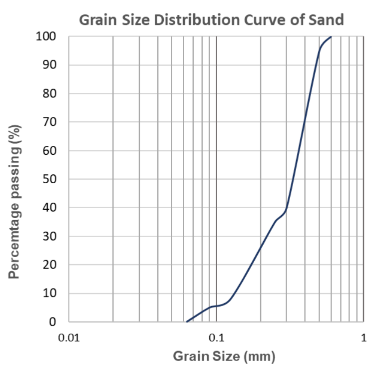

Particle Diameter (mm)	Amount in mixture (g)
0.500	100
0.300	550
0.250	50
0.125	270
0.090	30

The research aim includes testing various mixtures of differing proportions to evaluate the impact of the fine content on the test results, so six different mixtures were prepared. Each mixture consisted of nine samples separated into three batches of three samples each. One batch was subjected to FT cycling, denoted as ‘FT’, one was saturated at room temperature, denoted as ‘Saturated’, and one was tested dry, denoted as ‘Dry’. Each sample in a batch was tested with a different normal stress to compare with the other batches. The proportions per sample were decided based on the resources available and previous studies on the mechanical properties of sand and clay mixtures (K. Yin et al., 2021). Table 2 shows the proportions per sample of clay and sand.

Table 2: mixture proportions

Mixture	Amount of sand (%)	Amount of clay (%)	Nomenclature
1	30	70	30S/70K
2	40	60	40S/60K
3	50	50	50S/50K
4	80	20	80S/20K
5	90	10	90S/10K
6	95	5	95S/05K

Each sample was spooned into its own box. The shear boxes were measured and found to have a height of 3.4 cm, length of 6 cm and width of 6 cm, so the area of the boxes is 36 cm^2 and the volume is 115.20 cm^3. The boxes were filled up to a height of 3 cm with soil, so that the rest could be covered by a water film to fully saturate the samples, therefore each sample should have a total volume of approximately 72 cm^3. Furthermore, the soil was compacted in the shear box in a dry state to achieve a dense initial density state. This was done to reduce the amount and size of air-filled voids in the dry samples, which was hypothesised to consequently cause less swelling and shrinkage due to the saturation and temperature changes of the samples throughout the FT cycles.

The dry initial state of the samples consists of the unit weights, density and void ratio of the samples. Both soils were assumed to have a particle density of 2.6 g/cm^3 given a specific gravity of 2.6 (Lozada et al., 2015) and a density of water of 1.0 g/cm^3. The kaolin has a dry unit weight of 11.3 kN/m^3 and a saturated unit weight 25.5 kN/m^3 (Brinkgreve et al., 2007). The sand is assumed to have properties analogous to Fontainebleau Sand, therefore the dry unit weight is assumed to be 15.4-16 kN/m^3 and the saturated unit weight is 17.6-20 kN/m^3 (Siddiquee, n.d.). The void ratio is a measure of the voids in a soil sample, and is calculated as follows:

$$e= V_v / V_s= (V_T - V_s) / V_s \qquad \text{(Equation 4)}$$

Where V_v= volume of the voids (empty or filled with fluid), V_T = the volume of the container and V_s = the volume of solids.

The void ratio of the sand was measured and ranged from 0.517 to 0.788. However, the mixtures are expected to present higher void ratios, especially as the kaolin content increases.

For the Saturated and FT batches, per sample, a water film was added so that it would reach the top of the shear box. Then, each container was placed inside a vacuum bell until the sample stopped releasing air bubbles which would occur once the air was pushed out of the voids to fill them with water. After saturation, further mass and volume measurements were taken to measure the wet state of the samples and to account for mass and volume changes throughout the FT cycles.

After saturating, samples of the FT batch were subjected to two FT cycles, each consisting of 4 hours of freezing and overnight thawing. A commercial freezer was used, which reached a temperature of -6ºC. This amount of cycles was chosen under the assumption that one cycle would not cause a large enough impact on the soil to easily measure. The Saturated samples were directly tested once the saturation was complete and the excess water had evaporated or set in the mixture. The Dry samples were tested immediately.

The shear test was conducted using three different normal loads, one for each sample in a batch (FT, Saturated and Dry). These were 20N, 40N and 80N. Additionally, the hanger weight of the machine is 4.5 kg, or 44.15N. Therefore the applied loads were 64.15N, 84.15N and

124.15N. Dividing these by the area of the shear box, 36 cm^3, gives the normal stresses 17.82 kPa, 23.37 kPa and 34.48 kPa. The aim of the tests was to obtain a relation between the horizontal displacement and the shear force that would reach a peak value (the peak strength) and converge in a residual value. The maximum horizontal displacement was imposed at 6 mm, but was reduced in some samples to 4.5-5mm as they were seen to already converge at a residual stress value at these displacements.

The raw data was collected and processed to produce the results, detailed in the following section. Appendix I contains a diagram depicting the structure of all the data used in this project.

4. Results

This section details the experimental results obtained as explained in Section 3, *Experiment preparation & execution*. After initial samples of the mixtures 40S/60K and 30S/70K were prepared, it was discovered that they experienced excessive shrinkage and fell under the minimum height required to conduct the direct shear test. This was attributed to the high clay content of the samples, which greatly increased their expansive properties. Furthermore, these samples dried out throughout the stages of the FT cycles, creating cracks and becoming brittle and non-elastic, which would not have yielded accurate results in the shear tests. Mixtures with a fine content of more than 50% were therefore discarded, and the experiment proceeded with the remaining four.

4.1 Void ratios

Firstly, the void ratios of each mixture were measured to obtain the maximum e_{max} and the minimum e_{min}. These values for each mixture were plotted and shown in Figure 10. Note that these values correspond to dry soil, which could be different to saturated or FT-induced soil.

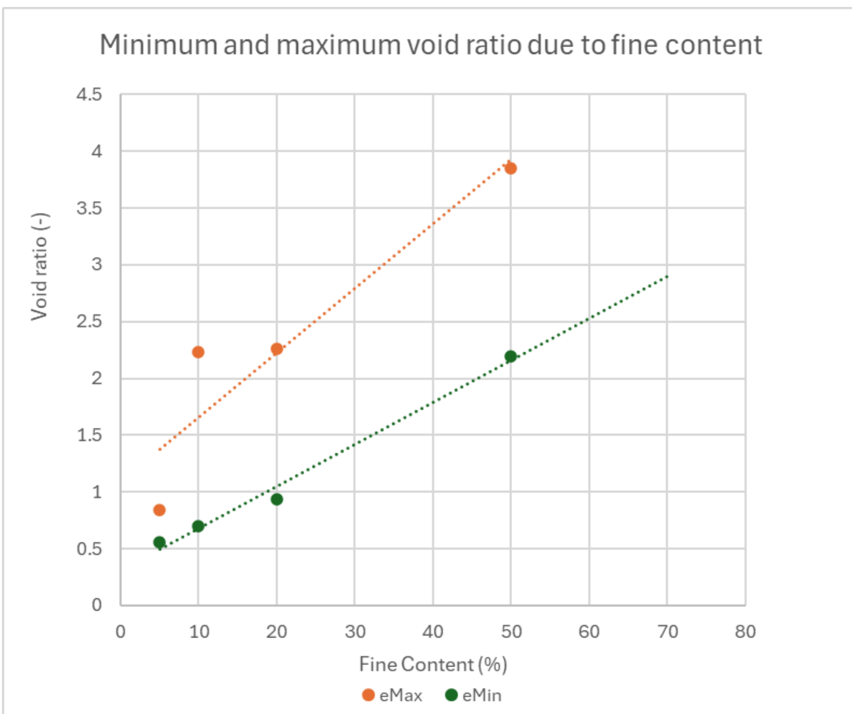

Figure 10: average void ratio per mixture fine content

As the fine content of the mixtures increases, so does the void ratio, showing how the presence of clay makes the grain configuration looser and more open. The void ratio of each sample subjected to FT cycling was measured throughout each stage of the sample preparation: dry, saturated, freezing 1, thawing 1, freezing 2, thawing 2. The numbering is used to represent the two FT cycles. These measurements were plotted for each sample, to show the changes in void ratio at every stage. Note that only samples subjected to FT cycling are included and all tested samples of this batch are plotted, where the discarded samples are depicted with a dotted line. These samples were discarded because the direct shear tests were faulty or inconclusive, either due to the results not attaining the desired values (both in sample height and peak strength) or major disruptions with excessive impact on the test results. The horizontal dotted lines denote the maximum (e_{max}) and minimum (e_{min}) void ratios in the dry state of the samples.

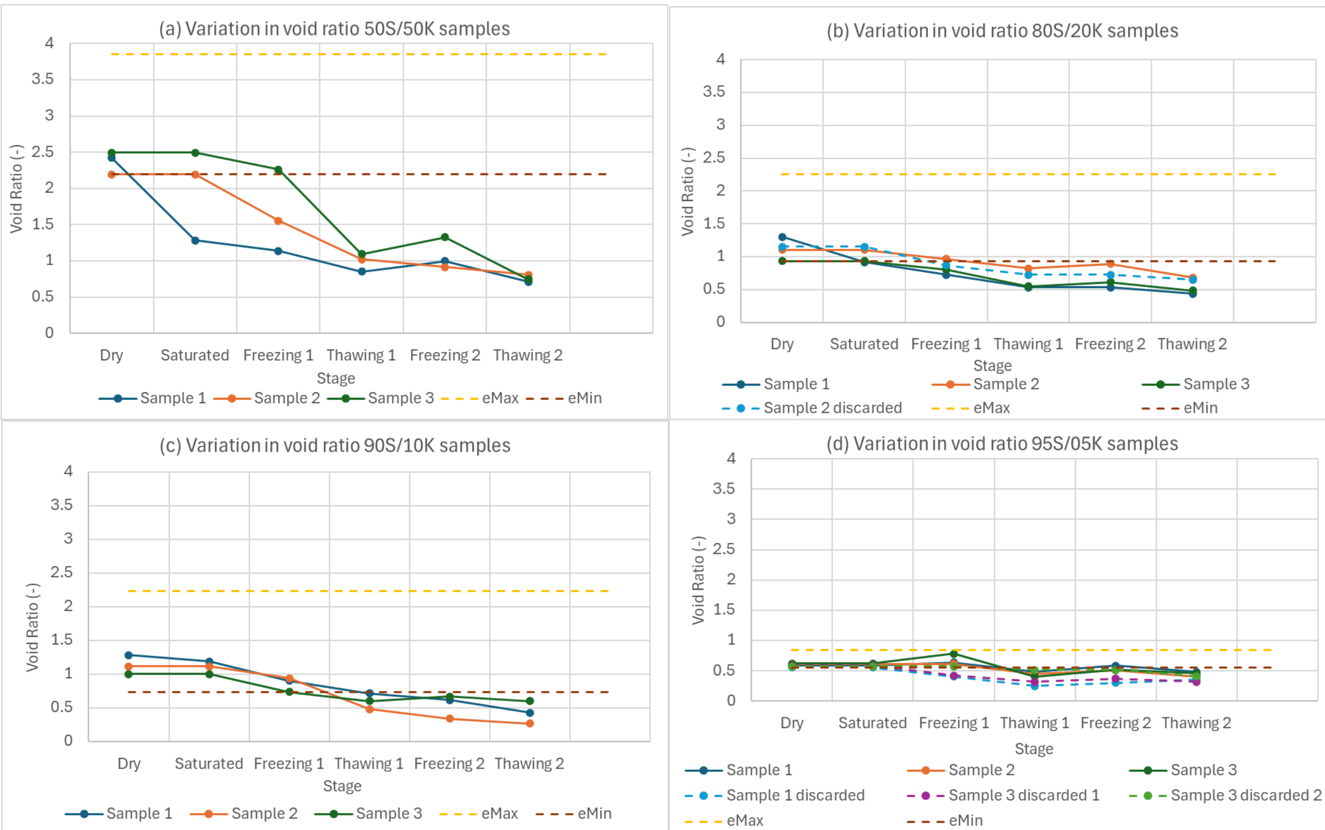

Figure 11: variation of void ratio per FT cycle stage per mixture. (a) 50S/50K mixture, (b) 80S/20K mixture, (c) 90S/10K mixture, (d) 95S/05K mixture.

There is a general trend for all mixtures of a decreasing void ratio as the stages go on, showing how the addition of water at the saturation stage causes further compaction of the soil, decreasing the volume of the voids. Frost heaving occurred at the freezing stages, but not for all samples and instances. The heaving is the largest in the 95S/05K mixture, which has the highest sand content. The sand has bigger pores and therefore a higher water content, meaning that the expansion during the freezing stages is bigger, and hence dilation is higher during freezing. However, theoretically more expansion should occur for a higher clay content, which implies the sample with high clay content experienced too much settlement upon saturation. Generally, more heaving occurs in the second freezing stage implying that repeated FT cycling causes a continuous increase in deformation of the soil and hence degrades it further. This aligns with the previously mentioned concerns of repeated cyclical freezing and thawing on the same soil.

4.2 Volume deformation

During the shearing stage of the test, the soil volume may vary where the soil can experience dilation or contraction. This depends on the initial density state of the soil (see Figure 5). The volume deformation of the soil during the shearing can be plotted against the horizontal displacement as in Figure 5 to show the soil's volumetric behaviour as it is sheared. Figures 12-15 show the plots of each mixture batch grouped by mixture. Note that these plots include only samples where the testing provided sound conclusions, therefore there are only 3 samples per mixture batch, each subjected to a different normal load as detailed in Section 3, *Experiment preparation & execution*.

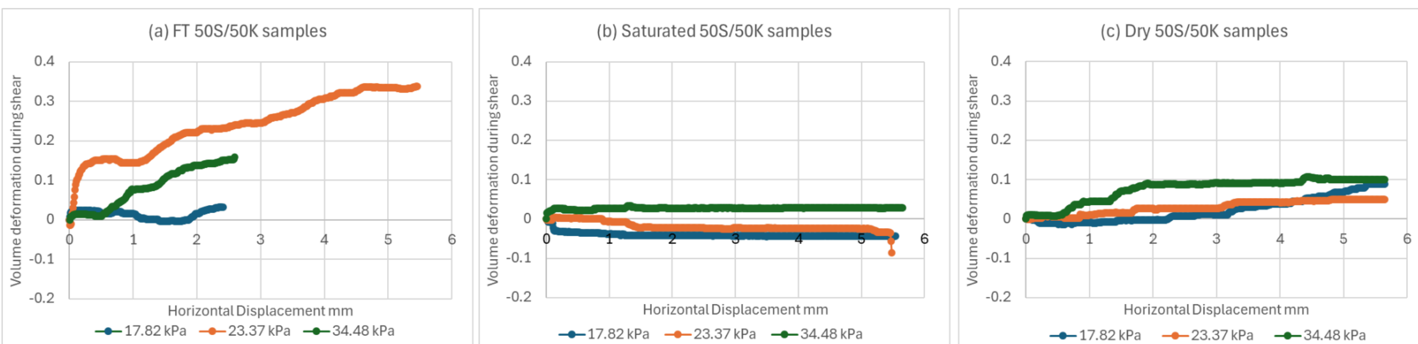

Figure 12: Volume deformation against horizontal displacement 50S/50K mixture. (a) shows the FT batch, (b) the saturated batch and (c) the dry batch.

The 50S/50K mixture generally showed dilation of the soil except for two samples of the saturated batch (blue and orange curves, graph (b)), which experienced minimal contraction. This shows that generally the samples had a dense initial state. The saturated samples might not have been as densely packed due to insufficient compaction when the preparation took place. In particular, the second sample of the FT batch (orange curve) showed the most dilation. Given by Figure 11 (a), the void ratio right before testing of this sample was 0.81 as opposed to 0.71 and 0.75 of the other two, which implies this sample was in a looser state. This defies the hypotheses made by Figure 5 on the soil density state due to the volumetric deformation during testing. Hence, some repetition of the tests with this mixture would help justify this occurrence.

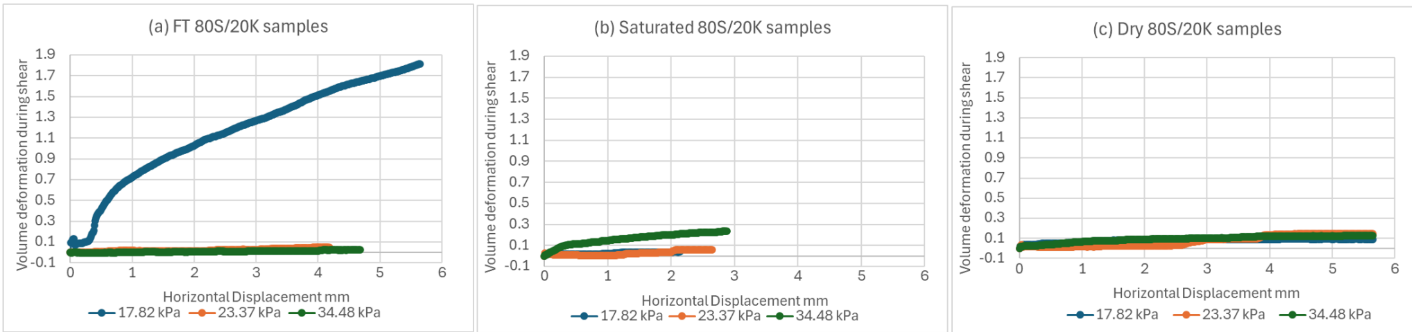

Figure 13: Volume deformation against horizontal displacement 80S/20K mixture. (a) shows the FT batch, (b) the saturated batch and (c) the dry batch.

In the case of the 80S/20K mixture, there is minimal dilation across the board excluding one sample of the FT batch that experienced significant dilation (blue curve in graph (a)). The void ratio of this sample right before testing is 0.44, compared to 0.68 and 0.48 of the second and third samples, which are represented by the orange and green curve respectively. This proves that the first sample was more compacted, albeit not much more than the third sample, so these results are still affected by randomness most likely due to this specific mixture's properties.
All the samples present a dense initial state as they all experienced dilation (as explained in Figure 5), which can be attributed to the compaction as well as the expansive properties of the mixture that further compacted due to the addition of water and volumetric alterations of the FT cycles.

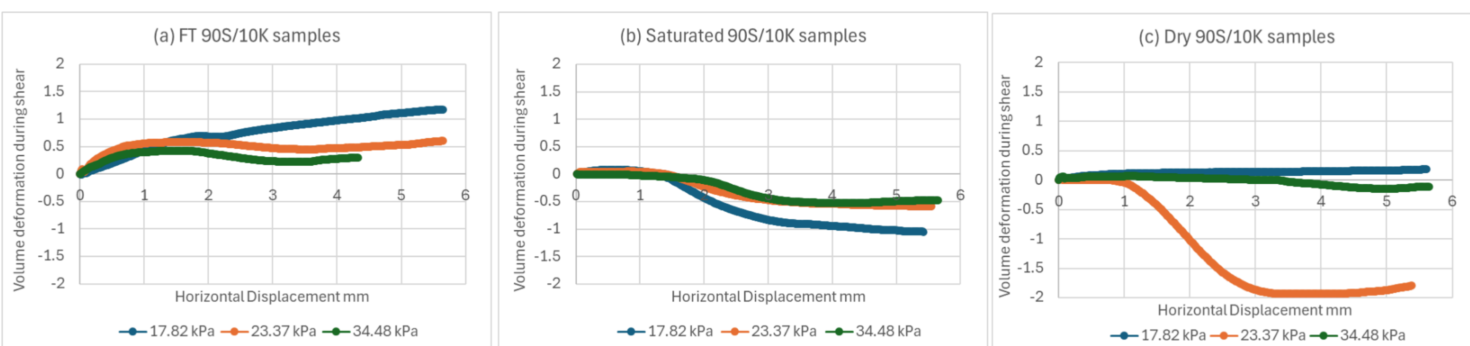

Figure 14: Volume deformation against horizontal displacement 90S/10K mixture. (a) shows the FT batch, (b) the saturated batch and (c) the dry batch.

The 90S/10K mixture shows inconsistent behaviour when comparing each batch of samples. For the FT batch it is clearly seen that dilation occurred, denoting a dense state that likely arose due to the combination of saturation and FT cycles. In the case of the saturated batch, the density state seems to have been mildly loose. The void ratios of this batch are 0.77, 0.81 and 0.75 for the blue, orange and green curves respectively. Figure 10 shows the minimum void ratio of the 90S/10K mixture to be around 0.70, so these samples present middling to low ratios explaining the mild contraction shown in Figure 14(b). Two out of the three dry samples follow a near horizontal trend (blue and green curves, graph (c)), while the third sample (orange curve) exhibits high contraction. This sample had a void ratio of 0.70 at testing, much lower than the 0.81 and 0.89 of the other two samples, therefore it was in a much looser state and contracted more as shown in Figure 14 (c).

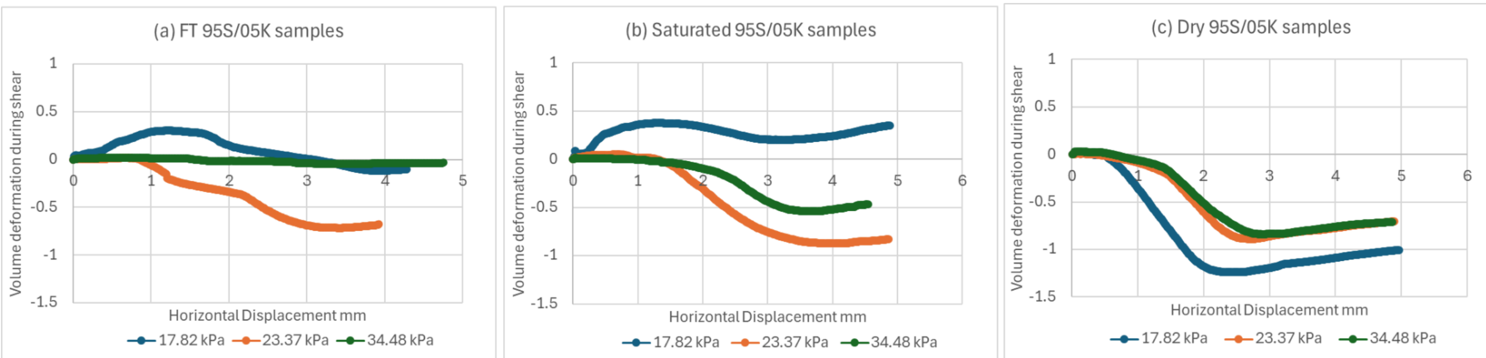

Figure 15: Volume deformation against horizontal displacement 95S/05K mixture. (a) shows the FT batch, (b) the saturated batch and (c) the dry batch.

The final mixture, 95S/05K overall presents more contraction of the soil, so a loose density state, except for some instances. In a dry state the void ratios range from 0.62 to 0.64, lying within the e_{max} and e_{min} of the dry 95S/05K mixture given by Figure 10, which are 0.84 and 0.56 respectively. In a saturated state, the range shifts slightly, to 0.62-0.66, so the contraction of this batch is less severe. However, the first sample (blue curve) shows high dilation, for a void ratio of 0.65, which is higher than that of the orange curve, 0.62, therefore the blue curve should lie below the orange curve based on the theory. This anomaly also opposes the theory described by Figure 5.

The FT batch has void ratios ranging from 0.40 to 0.48, so based on the theory it is expected these would contract less than the Saturated and Dry batches, however this did not always occur. Sample 1 of the FT batch (blue curve of graph (a)) shows dilation at first, but gradually falls to minimal contraction. This can be due to a change in the density state during testing, where for example water inside the mixture was expelled as the shearing occurred loosening the density state of the mixture and leading to contraction.

Overall, the results demonstrate that in the FT state the dilation is larger for higher clay content. The changes in void ratio per stage (Figure 11) show that the mixtures with high clay content had a very high void ratio in dry state and decreased substantially throughout the FT cycles. In general, the more fine content that was present the bigger this decrease was (the curves are steeper for 50% and 20% clay). Thus generally the samples were more dense as the fine content increased if subjected to FT cycling. It was also observed that in a dry state, there was more contraction for a higher amount of sand, clearly because the sand is considerably denser than the clay.

4.3 Shear stress

Direct shear tests are generally performed to assess the shear strength characteristics of the soil. Figures 16-19 show the relationship between the shear stress and the horizontal displacement during the shearing stage of the test. As described in Section 2.1, [Problem Context](), the shear strength is expected to be greater for dry samples and for greater normal stresses. Therefore, the peak values should increase for increasing normal loads and be higher for dry samples.

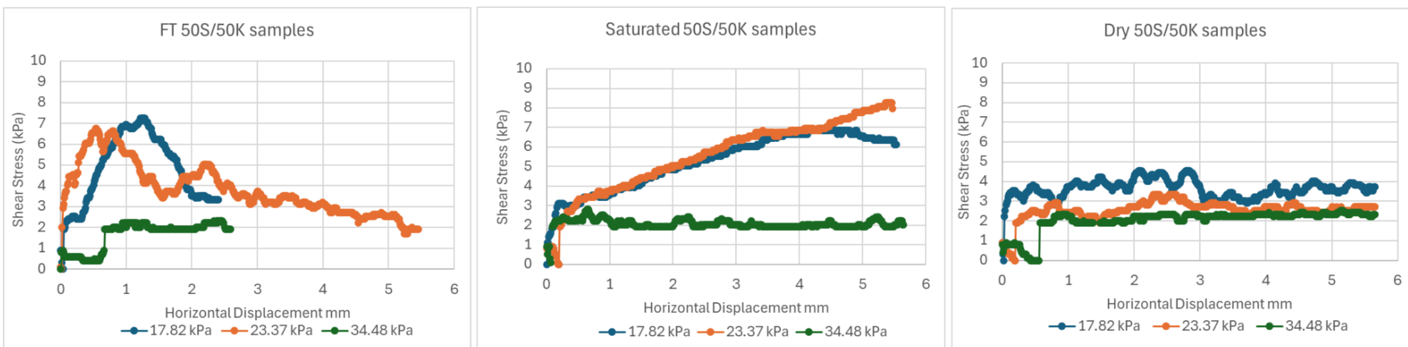

Figure 16: Shear stress against horizontal displacement 50S/50K mixture. (a) shows the FT batch, (b) the saturated batch and (c) the dry batch.

The 50S/50K mixture showed no alignment with the hypothesised behaviour, sometimes in fact showing the opposite behaviour, where the peak strength decreased under increasing normal loading. This discrepancy may be caused by the reduction in height due to saturation, FT cycles when present, and the application of the vertical loads, which eventually lead the samples to fall under the minimum required height for proper testing (half of the shear box height), so the samples could not be properly sheared. It is not clear what the cause of this was, since it happened regardless of the state of the samples (dry, saturated or FT), therefore further research could focus on investigating this phenomenon and discerning whether it was a result of the experiment preparation, or if it was the natural behaviour of the soil mixture.

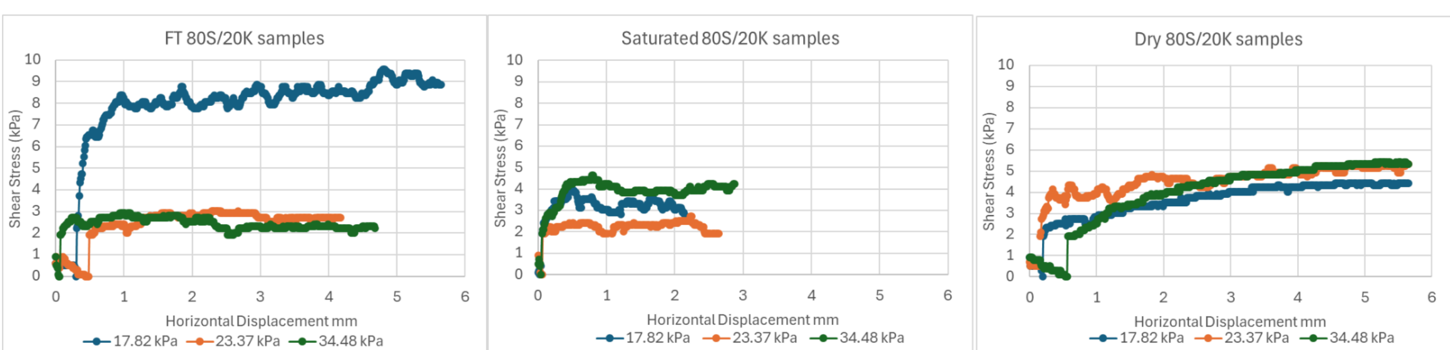

Figure 17: Shear stress against horizontal displacement 80S/20K mixture. (a) shows the FT batch, (b) the saturated batch and (c) the dry batch.

The same situation is present for the 80S/20K mixture, where similar issues of excessive collapse and inadequate shearing affected the test results. This leads to the conclusion that further repetition is required to justify these trends or to achieve the hypothesised trends. The conclusion can also be made that a fine content of 20% or more leads to this unexpected behaviour, therefore more repetitions could also test this assumption.

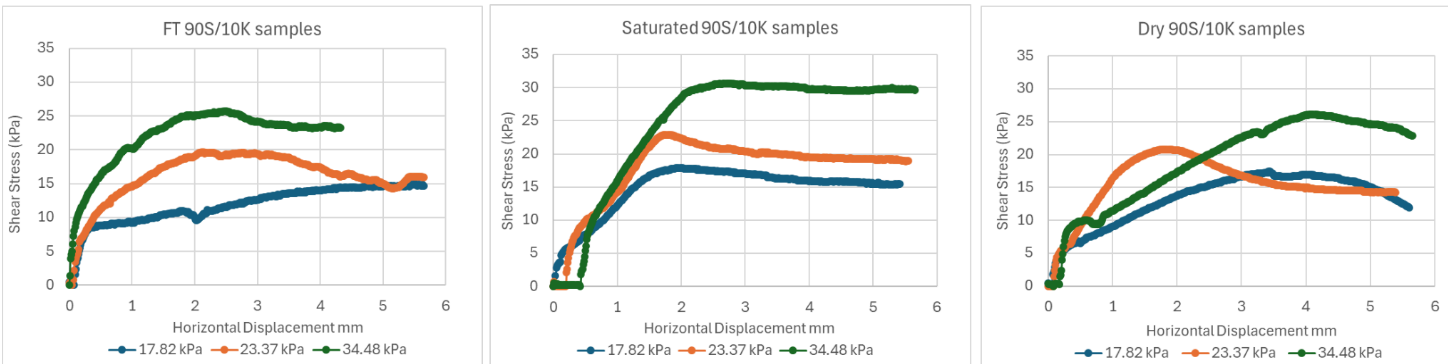

Figure 18: Shear stress against horizontal displacement 90S/10K mixture. (a) shows the FT batch, (b) the saturated batch and (c) the dry batch.

The 90S/10K starts to produce adequate results, with defined peaks at considerably high values of shear stress. It is seen that the peaks become sharper when moving from left to right, implying that the FT cycling flattens the peak strength. The peaks are also displaced, but not all in a uniform way. Two samples of the dry batch peak much later than the other batches, while the remaining one peaks much earlier. This could be due to the mixing of the soil and the distribution of the pore water pressure across the mixtures. It is also seen that the peaks are not necessarily higher for the dry batch but are quite similar to the other batches. Therefore the FT cycling was not sufficient to show noticeable effects. Furthermore, this mixture presented quite erratic behaviour, as seen by the many repetitions of especially the saturated batch, where the shear stress values greatly depended on the water content.

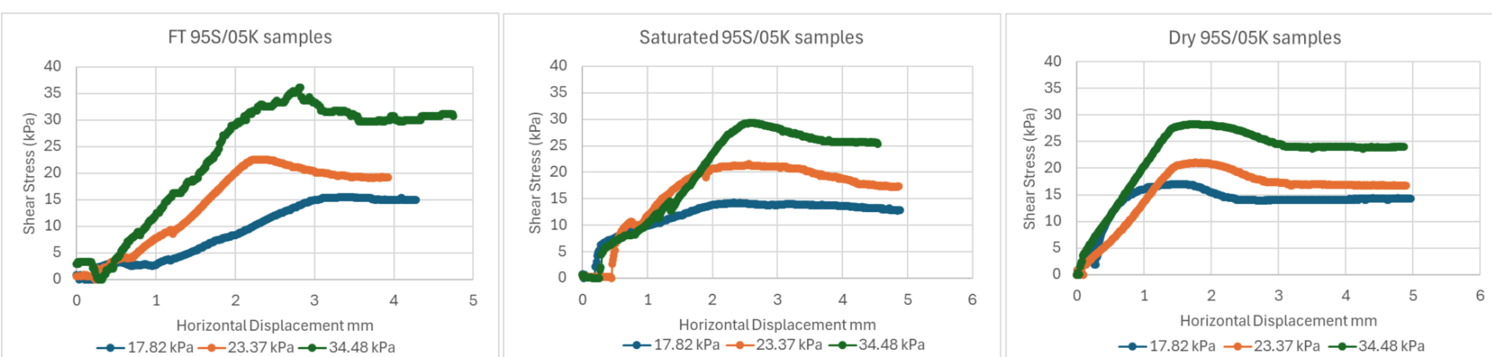

Figure 19: Shear stress against horizontal displacement 95S/05K mixture. (a) shows the FT batch, (b) the saturated batch and (c) the dry batch.

Mixture 95S/05K shows similar results to the previous mixture, again indicating that a fine content of below 20% yields consistent results that match the literature. Peak mobilisation occurs, but this time it is more noticeable with the dry samples peaking up to 1 mm before the FT samples and the saturated samples peaking somewhere between the two. This depicts a clear trend of a leftwise movement of the peak as the soil is subjected to further saturation and FT cycling. The same situation occurs in terms of peak values when comparing the batches, where the dry batch does not necessarily have a higher value. In fact, sample three of the FT batch (green curve, graph (a)) shows the highest peak. This could have been due to movement of the soil inside the gap between both halves of the shear box, which added extra friction to the shearing and thus altered the results.

4.4 Yield loci

Having plotted the shear stress, the yield loci of the samples can be drawn, using the peak strengths and the imposed normal stresses to create the mixtures' failure envelopes. Figure 20 shows each mixture's yield loci, one for each mixture batch (FT, saturated and dry). As discussed in Section 2.4, *Research Methodology*, the yield locus of a batch of samples should follow a linear upward (positive gradient) trend, to show how the peak strength increases with increasing normal stress. Furthermore, it is expected for yield loci of batches of dry and saturated samples to lie above the loci for FT samples, given the literature discussed in Section 2.1, *Problem Context*.

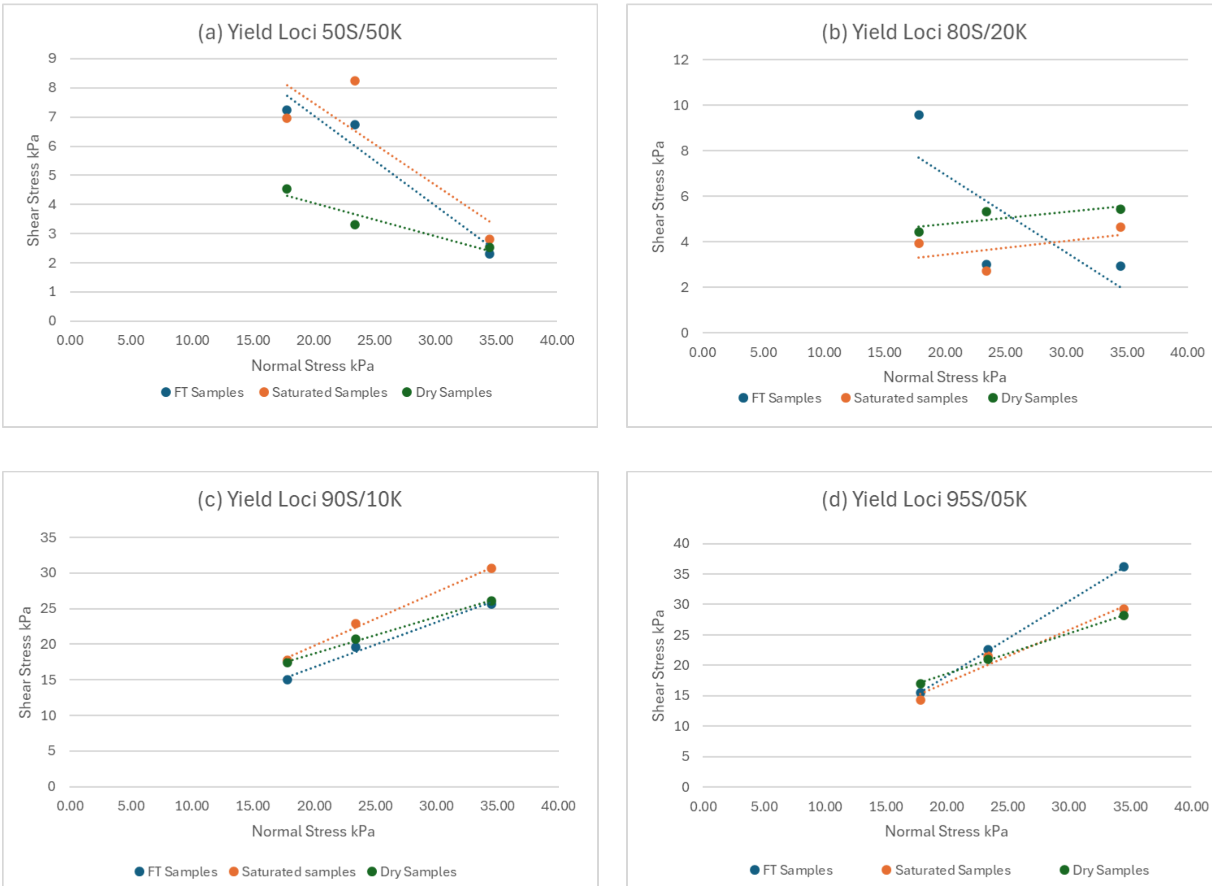

Figure 20: Yield loci of every soil mixture. (a)50S/50K mixture, (b)80S/20K mixture, (c)90S/10K mixture, (d)95S/05K mixture

As shown above, only two mixtures built a proper set of yield loci, being the mixtures with less fine content. As explained in Section 4.3, *Shear stress* and shown by the results, the shear stress variation of the mixtures with higher fine content did not exhibit the expected behaviour, with more normal stress leading to lower peak strengths. This is likely due to the issue of insufficient height of the samples. However, it could be attributed to issues in the acquisition and processing of the data or the preparation and execution of the experiment.

In the 90S/10K mixture, the yield locus of the saturated batch is the highest one, so this batch presented higher peak strengths across the board. For the 95S/05K mixture, the FT batch has the highest locus. This suggests insufficient compaction of the dry batch. Looking at the void ratios, the dry batch ranged from 0.63 to 0.64, which lies within the range of the saturated batch, 0.62-0.66 and above the FT batch, 0.40-0.48. Theoretically, the FT batch has the lower void ratios and should therefore lie below the other batches. The saturated and dry batches would be intertwined, given that the void ratio ranges intersect. However, this is not the case, which suggests additional issues with the elaboration and collection of the data. As mentioned under Figure 19, movement of the soil inside the gap of the shear box created additional friction and is most likely because of these anomalies.

This also suggests that the degree of FT cycling was not sufficient to cause noticeable impact on the samples and provide desired results. Therefore, more FT cycles or lower temperatures might be needed.

4.5 Cohesion and friction angle

The yield loci can be best fitted by the Mohr-Coulomb linear criterion (see Equation 2). Therefore, these equations give the friction angle (arctangent of the gradient) and cohesion (y-intercept) of the sample batches. These can be compared to see the impact of the fine content and the FT cycling on these fundamental properties. Tables 3 and 4 show these values per mixture. Only the 90S/10K and 95S/05K mixtures will be discussed in this section, given that these mixtures followed the desired trends. See Appendix II for the tables of the 80S/20K and 50S/50K mixtures. Since these presented negative values for friction angle, which has no physical meaning, further research and different approaches are therefore recommended.

Table 3: Cohesion and friction angle of 90S/10K mixture

Batch	**Equation of trendline**	**Friction angle (degrees)**	**Cohesion (-)**
FT	y= 0.6267x + 4.30	32.08	4.30
Saturated	y = 0.7575x + 4.66	37.14	4.66
Dry	y = 0.5141x + 8.45	27.21	8.45

The 90S/10K mixture showed larger cohesion for the dry batch, showing how this batch had higher internal strength of the particles and how this was reduced by the addition of water. The closeness in results between the saturated and FT batches once again shows that the degree of FT cycling might have not been sufficient to present highly different results.

Table 4: Cohesion and friction angle of 95S/05K mixture

Batch	**Equation of trendline**	**Friction angle (degrees)**	**Cohesion (-)**
FT	y= 1.2368x + 0	51.04	0
Saturated	y = 0.8715x + 0	41.07	0
Dry	y = 0.6669x + 5.27	33.70	5.27

Finally, the 95S mixture shows a similar trend in cohesion as the 90S/10K mixture, but an opposite one in friction angle. As explained in Section 4.3, *Shear stress*, the higher friction angle of the FT batch might be due to the movement of soil between the halves of the shear box that created additional unwanted friction. Therefore, and assuming the trends of the 90S/10K mixture should be present in this mixture as well, more repetition could achieve this or support the trends shown in Table 4.

The cohesion and friction angle were plotted against the percentage of fine content to show how these properties are influenced by the percentage of fine content. Similarly to the yield locus, the change in cohesion is expected to follow a linear upward trend because the clay is highly cohesive, so a larger fine content increases cohesion. Meanwhile, the change in friction angle is expected to follow a downward trend, since a higher clay content supposes a lower friction angle of the mixture as the clay has a low frictional shear resistance. Moreover, the FT batches should exhibit lower values of cohesion and friction angle than the rest and the dry batches should exhibit higher values.

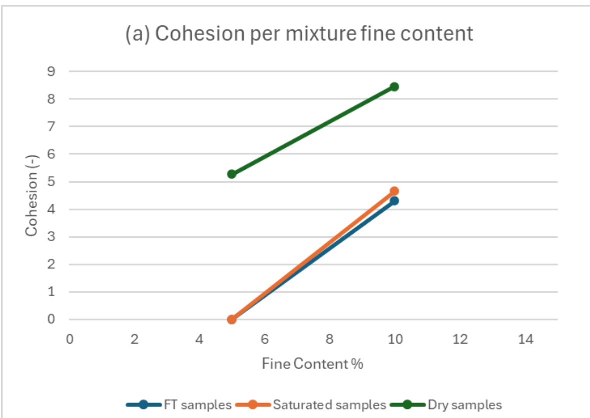

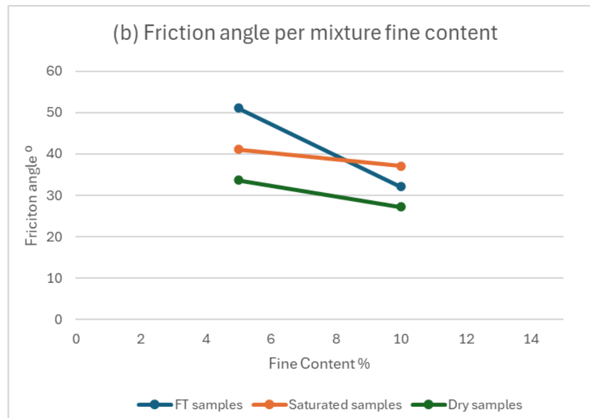

Figure 21: (a) plot of cohesion against percentage of fine content. (b) plot of friction angle against fine content

The cohesion graph follows exactly the desired trends. The difference between the saturated and FT batches is barely visible while the difference from the dry batch is quite large, especially for a fine content of 5%. This suggests that the addition of water significantly reduces the cohesion of the soil, thus reducing the non-frictional shear resistance. This is shown to be more severe for lower fine contents.

In terms of the friction angle, the trend indeed has a downward trajectory, but it does not follow the expectations about the difference between the batches. The dry batch presents the lower friction angles, which indicates this batch had a lower shear resistance due to friction. For 5% fine content, the FT batch shows the highest friction angle, which again could result from the movement of soil between the halves of the shear box providing additional friction. For 10% fine content the saturated batch has the higher friction angle instead, so this is not consistent unlike in the cohesion graph. This might also indicate that the degree of FT cycling was not strong enough to yield the desired results.

Generally, the results suggest that the soil mixtures have a lower non-frictional shear resistance and a higher frictional resistance as the fine content decreases, aligning with the known behaviour of sand and clay.

Finally, the cohesion and friction angle were also plotted against the average void ratio per mixture batch right before testing, to further investigate the influence of the saturation and FT cycling on the shear strength characteristics.

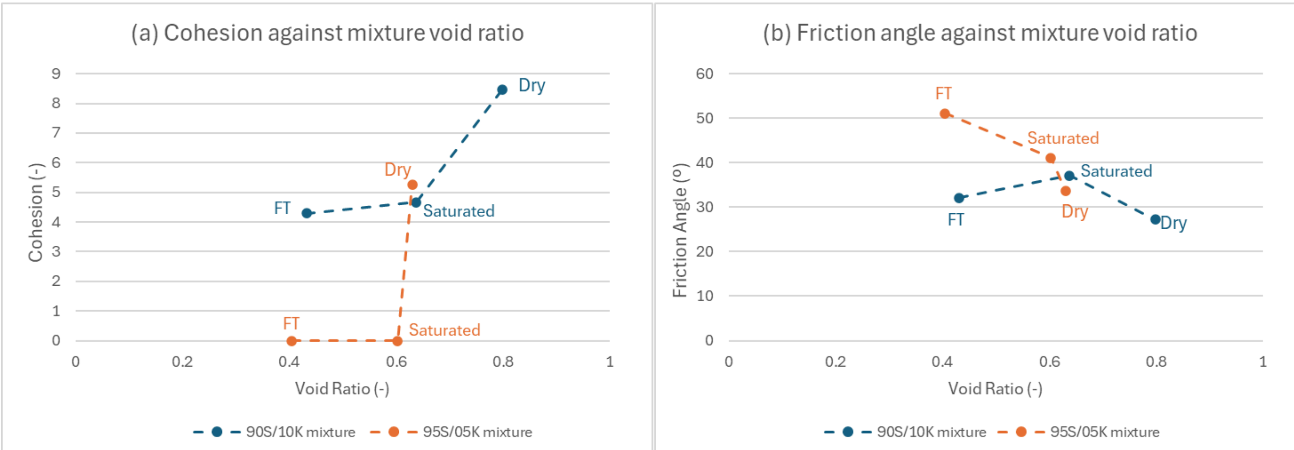

Figure 22: (a) cohesion against average void ratio. (b) friction angle against average void ratio

Void ratio and cohesion theoretically have an inversely proportional relation. Cohesion is related to the degree of contact between particles, so a higher void ratio indicates more space between the particles and less contact. However, Figure 22 (a) does not demonstrate this. While it does correctly show that the void ratio is lower for the FT and saturated batches relative to the dry one, showing the effects of FT cycling and saturation on the soil volume, the cohesion seems to increase for increasing void ratios. This suggests that although the dry batch has a higher void ratio, the FT cycling and saturation cause a decrease in the cohesion that is more notable than the index of the void ratio.

In terms of the friction angle, an inversely proportional relation is expected as well. This is achieved partially, as a general decrease in friction angle is seen as the void ratio increases, except for the saturated batch of the 90S/10K mixture where an increase is seen. Despite this anomaly, it can be deduced from the results that saturation increases the friction angle. This is because saturation was shown to reduce the void ratio (see Figure 11), which reduces the size of the voids and brings solid particles together, increasing the overall friction between them.

These results imply that saturated soils have a lower non-frictional shear resistance, but a higher frictional resistance. The latter goes against the hypothesis that FT cycling and saturation decrease the shear strength of the soil, but given that the shear strength is intrinsically linked to many other soil properties, there may be additional properties that bring about the results shown.

5. Discussion

The results of the experiment will be discussed and reflected upon in light of the research questions posed in Section 2.3.2, *Research Questions*. This section will be structured based on these research questions.

Firstly, this project aimed to understand which initial conditions of the soil have the greatest impact on the mechanical properties of the soil. In particular, the initial density state and the amount of fine content in the soil were investigated. The density state of the soil dictated if the soil experienced dilation or contraction during shearing. This occurrence was expected to follow a trend based on theory described in Figure 5. However, there were discrepancies present, where the void ratio of specific samples indicated a specific density state that did not align with the volumetric deformation exhibited by the shear tests.

In terms of the volume deformation, it was seen that the majority of the samples with high clay content were in a dense state. It was also observed that in the FT state there was more dilation as the fine content increased. This was backed up by the variations in void ratio throughout the FT stages, which showed that the drop in void ratio was more extreme as the fine content increased (see Figure 11), meaning the samples compacted more and became denser. These observations indicate that samples with high fine content were denser due to the effects of the FT cycling.

On the contrary, in the dry state, there was more contraction as the sand content increased. Clearly this is because the sand is more loose than the clay and there were no additions such as water or induced freezing, so the samples did not compact any further after preparation. The void ratios and density state remained constant.

When examining the shear strength evolution, most of the samples with high fine content do not show a defined peak nor do they converge at a residual value, but rather oscillate around a relatively low value in comparison to the low fine content mixtures. This can be traced back to the fact that samples with higher fine content were seen to contract more when normal load was applied, and possibly shrunk below half of the height of the shear box (see Section 2.4, *Research Methodology*) affecting the results. Therefore, a comparison between these and the volume deformation results is not possible and further repetition of the tests is required to elaborate on it.

The mixtures with low fine content also show discrepancies between contractive and dilatant response when comparing the shear strength and the volume deformation, especially for saturated and dry samples.

The fine content had very noticeable effects on the mechanical response. Evidently, the higher the fine content, the higher the initial void ratio, with less variation throughout the saturation, freezing and thawing stages. Kaolin is a very fine and lightweight clay that occupies a large volume with relatively little mass, demonstrated by the larger void ratio. In terms of the shear strength, the more fine content in the samples resulted in more inconsistent and random variations, which also did not fit the literature (see Figure 4). It was expected that in every case, a higher normal load would result in higher peak strength, but the opposite happened with the 50S/50K and 80S/20K. This can be clarified once again by the issue of excess contraction when normal loading was applied, which rendered the results of the shearing stage undesirable.

The second research question concerned the impact of the FT cycles on the shear strength of the soil mixtures specifically. It was hypothesised that the peak strength would decrease and be mobilised for samples with induced FT cycling. The test results show that this only happened partially. In the case of a lower peak strength, when examining the yield loci, the 90S/10K mixture clearly shows how the samples with FT cycling had a lower peak strength across the board. In the case of the 95S/05K mixture, this does not quite happen, especially due to the third FT sample peaking higher than the rest. This could be due to the FT cycling not being sufficient enough to create noticeable changes in the samples.

Although one mixture behaved as expected, the change is still quite small, so it is recommended to consider undergoing more cycles or lowering the freezing temperature to produce more visible degradation and heaving of the soil. Furthermore, the result for the 95S/05K mixture implies that more sand requires a more intense FT cycling to produce distinct results.

Mobilisation of the peak is clear in the 95S/05K mixture, with the dry samples peaking up to 1mm before the saturated and FT samples. The 90S/10K mixture showed mobilisation in the opposite end, with the dry samples peaking much later than the saturated and FT samples, but this is not consistent for all.

Additionally for this mixture, the peaks look sharper in a dry state and seem to flatten due to the saturation and even more due to the FT cycling. Meanwhile, the 95S/05K mixture shows almost always relatively sharp peaks, but especially the dry batch converges very uniformly to a residual value, inferring that the combination of high sand content and undisturbed material yields the most alike relationship to the studied literature.

It was expected that the Mohr-Coulomb criterion would demonstrate the shear strength degradation, by showing the yield loci of the FT samples lying vertically below the saturated and dry samples. This was not always the case, but it did serve as a clear indication of the relative failure envelope of each batch of samples. It is possible that this could have been achieved by a higher degree of FT cycling, either due to colder temperatures or a higher number of cycles. However, the cohesion and friction angle of the sample batches yielded unreasonable results that were not fit for the analysis on the mixtures with high fine content specifically. This is probably a result of the aforementioned excessive contraction of the soil, but if this behaviour is natural for these mixtures it could suggest that the Mohr-Coulomb criterion is not optimal to depict their behaviour. Nonetheless, it is most certainly an issue of the sample used and not the soil’s natural behaviour. Therefore, with additional analyses of different degrees of FT cycling, the Mohr-Coulomb criterion can even more optimally depict the decrease in strength properties due to FT cycling. When comparing the cohesion and friction angle with the void ratio at the time of testing, there seemed to be a strong indication that saturation increases the frictional shear resistance, but reduces the non-frictional shear resistance. The latter seems to then take precedence in the overall reduction of shear strength, but further repetitions or a wider scope can give more insight into exactly which of these properties is the factor in the reduction of shear strength due to saturation and FT cycling.

When looking at the described literature, inaccuracies are present in the yield loci and peak strengths, the volume deformation and the cohesion and friction angle. The yield loci were all expected to follow a linear upward trend, but this was only achieved fully for half of the mixtures, and only partially for the other half. During testing the mixtures with higher fine content seemed to collapse very easily and were overall weaker in strength than the mixtures with low fine content. The sample preparation might have been the issue, in particular the compaction of the soil and the saturation. While the methods used worked for some mixtures, they did for others. So, it is recommended to tailor the sample preparation process to each specific mixture to achieve more desirable results.

The peak strengths were expected to reduce as saturation and FT cycling were induced, but this was not always the case. The volume deformation was not always in line with the shear strength evolution to describe the soil density state, but this comparison was not always possible due to the excess contraction. Results in the cohesion and friction angle were the most undesirable, since only half of the mixtures properly fit the Mohr-Coulomb criterion.

The amount of water required to saturate the samples had to be different for each mixture due to the amount of fine content, which at times led to excess water being added, triggering liquefaction of the samples that rendered them too weak to properly measure the shear strength. When this occurred, the samples were discarded, but it may still have had an impact, albeit small, on the samples that were reported and analysed.

Also, in some instances water leakage through the gaps of the shear box occurred, which also transported some material away from the mixture, leading to slight errors in mass measurements. The leakage was fixed by patching up the shear boxes with silicone before spooning in the samples, but this did not always stop minimal leakage from occurring.

There might also be some uncertainty in the void ratio variation of Figure 11, since the void ratios at the saturated state were not properly measured. The height of the samples was first measured with the height of the water film, but this should not have been included. In the end the height at saturation was assumed to be the same as the height in dry state, which is likely not the case in practice. Moreover, when the test began, one sample of each mixture was prepared. This first round of samples was not compacted, as it was initially decided not to compact, and this decision was changed after preparing these samples and omitting the 30S/70K and 40S/60K mixtures. Therefore, each mixture has a sample with a discrepant void ratio value that is not fully comparable with the rest of the samples in the mixture.

Overall, the analysis did not completely fit the hypotheses drawn from the literature, mainly due to unwanted occurrences during testing and issues with the experiment preparation, execution and processing of the data. Based on the findings and the uncertainties identified, further research can incorporate these to update the analysis and either produce the desired results or justify some of the unusual trends discovered in this report.

6. Conclusion

To conclude, the project aimed to understand the impact of induced FT cycling on the mechanical response of soil mixtures. The focus was on the shear strength and related characteristics such as volume deformation, and void ratios.

The results indicated that soil mixtures with higher fine content showed more inconsistent and unpredictable behaviour, often deviating from expected trends. On the contrary, mixtures with lower fine content showed more uniform results, but they did not always align with the hypotheses made based on the literature.

The FT cycles generally led to a reduction in peak shear strength, but the extent of this effect varied across the different mixtures. The 90S/10K mixture demonstrated the most notable decrease in peak strength due to FT cycling, while the 95S/05K mixture showed the most mobilisation of the peak strength, suggesting that the degree of FT cycling was not sufficient to yield significant changes.

The study also investigated the impact of the initial soil density and fine content on the shear strength characteristics of the mixtures. Higher fine content resulted in higher initial void ratios but also more extreme reductions in void ratio throughout the stages of the FT cycles. The findings suggest that inducing FT cycling at lower temperatures or a higher number of cycles is needed to produce more observable effects that better match the literature studied.

Overall, the experiment gave insight into the behaviour of soil mixtures due to saturation and induced FT cycling as well as during the direct shear test. However, the results did not desirably match the expectations set out by the problem context, leading to the recommendation of carrying out further research to reinforce the observed phenomena. In particular, this research could focus more deeply on shear testing of mixtures with high fine content, or on inducing higher degrees of FT cycling as aforementioned. It is also recommended to drive the focus of the sample preparation on the measurement of the void ratios, as these proved to be the main factor that rationalized many of the findings.

7. Bibliography

Brian, J. (2019, March 6). Direct shear test; to determine shear strength of soil. *CivilSeek*. https://civilseek.com/direct-shear-test/#google_vignette

Brinkgreve, R., Kappert, M., & Bonnier, P. (2007). Hysteretic damping in a small-strain stiffness model. In *Taylor & Francis eBooks*. https://doi.org/10.1201/noe0415440271.ch106

De Guzman, E. M. B., Stafford, D., Alfaro, M., Doré, G., & Arenson, L. U. (2018). Large-scale direct shear testing of compacted frozen soil under freezing and thawing conditions. *Cold Regions Science and Technology*, *151*, 138–147. https://doi.org/10.1016/j.coldregions.2018.03.011

Head, K. H., & Epps, R. (2011). *Manual of Soil Laboratory Testing vol II 3rd edition, Vol. II: Permeability, Shear Strength and Compressibility Tests*. White Publishing. https://www.whittlespublishing.com/Manual_of_Soil_Laboratory_Testing_Vol_II

Hossain, M. S., PhD PE, Islam, M. A., Badhon, F. F., & Imtiaz, T. (2021, January 14). *Direct shear test*. Pressbooks. https://uta.pressbooks.pub/soilmechanics/chapter/direct-shear-test/

Kadivar, M., & Manahiloh, K. N. (2019). Revisiting parameters that dictate the mechanical behavior of frozen soils. *Cold Regions Science and Technology*, *163*, 34–43. https://doi.org/10.1016/j.coldregions.2019.04.005

Lozada, C., Caicedo, B., & Thorel, L. (2015). Effects of cracks and desiccation on the bearing capacity of soil deposits. *Géotechnique Letters*, *5*(3), 112–117. https://doi.org/10.1680/jgele.15.00021

Mishra, G. (2017, December 18). *Types of shear failure of foundation on soils*. The Constructor. https://theconstructor.org/geotechnical/types-of-shear-failure-of-foundation-soils/7492/#google_vignette

Murton, J. B. (2021). Periglacial processes and deposits. In *Elsevier eBooks* (pp. 857–875). https://doi.org/10.1016/b978-0-12-409548-9.11925-6

Obinna, U. (2021, August 29). *Stress Path Approach for Shear Strength of Soils - Structville*. Structville. https://structville.com/2021/08/stress-path-approach.html?expand_article=1

Prasad. (2023, May 25). *Cohesion of Soil | Geotechnical Engineering*. Structural Guide. https://www.structuralguide.com/cohesion-of-soil/#:~:text=Cohesion%20of%20soil%20refers%20to%20the%20internal%20strength,that%20enables%20the%20soil%20to%20resist%20shear%20forces.

Pratik. (2023, October 16). Mohr's circle explained, Learn how to draw it. *Mech Content*. https://mechcontent.com/draw-mohrs-circle/

Shastri, A. M., Sánchez, M., Gai, X., Lee, M. Y., & Dewers, T. (2021). Mechanical behavior of frozen soils: Experimental investigation and numerical modeling. *Computers and Geotechnics*, *138*, 104361. https://doi.org/10.1016/j.compgeo.2021.104361

Siddiquee, T. (n.d.). *Sand unit weight or specific weight - calculation*. Civil Engineering. https://civiltoday.com/civil-engineering-materials/sand/360-unit-weight-of-sand

Sun, Z., Zhang, S., Wang, Y., Bai, R., & Li, S. (2022). Mechanical behavior and microstructural evolution of frozen soils under the combination of confining pressure and water content. *Engineering Geology*, *308*, 106819. https://doi.org/10.1016/j.enggeo.2022.106819

Tang, L., Cong, S., Li, G., Xue, L., & Gan, F. (2018). The effect of freeze-thaw cycling on the mechanical properties of expansive soils. *Cold Regions Science and Technology*, *145*, 197–207. https://doi.org/10.1016/j.coldregions.2017.10.004

User, S. (2013, September 14). *Angle of friction*. Copyright (C) 2024 My Site. https://www.geotechdata.info/parameter/angle-of-friction

Xu, X., Bai, R., Lai, Y., Zhang, M., & Ren, J. (2020). Work conjugate stress and strain variables for unsaturated frozen soils. *Journal of Hydrology*, *582*, 124537. https://doi.org/10.1016/j.jhydrol.2019.124537

Yin, K., Fauchille, A., Di Filippo, E., Kotronis, P., & Sciarra, G. (2021). A review of Sand–Clay Mixture and Soil–Structure Interface Direct Shear test. *Geotechnics*, *1*(2), 260–306. https://doi.org/10.3390/geotechnics1020014

Yin, Z., Hicher, P., & Jin, Y. (2020). Constitutive Relations of Saturated Soils: An Overview. In *Springer eBooks* (pp. 1–46). https://doi.org/10.1007/978-981-15-6307-2_1

8. Appendices

8.1 Appendix I: Data Management Plan

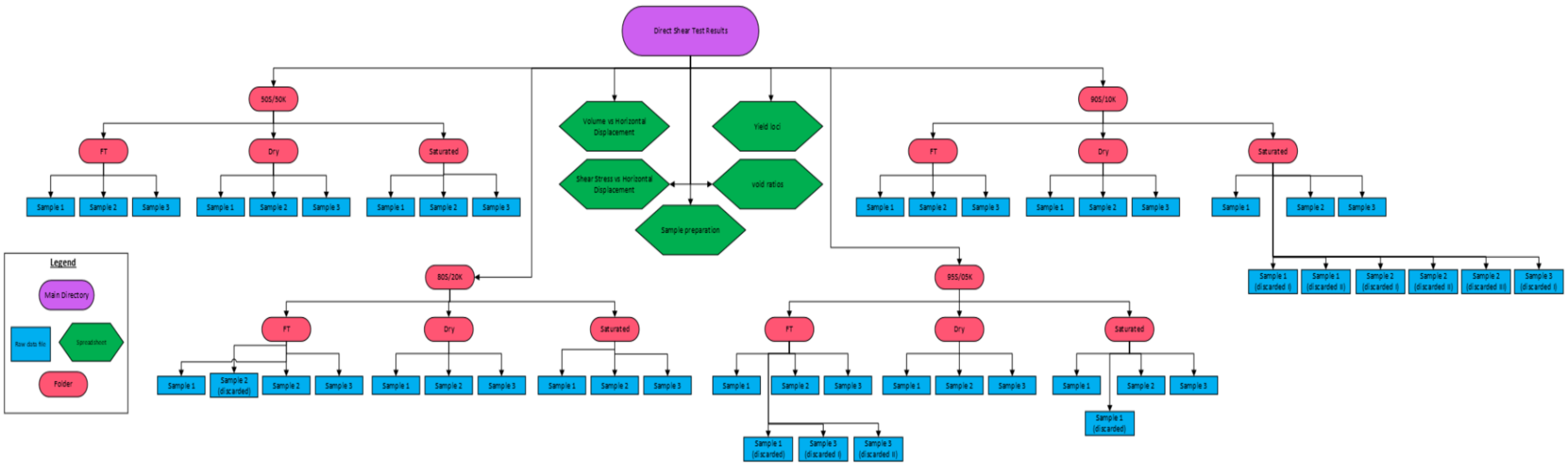

Figure 3: Data Management Plan diagram

8.2 Appendix II: Cohesion and friction angle of high fine content mixtures

Table 5: Cohesion and friction angle of 50S/50K mixture

Batch	**Equation of trendline**	**Friction angle (degrees)**	**Cohesion (-)**
FT	y = -0.3108x + 13.28	-17.27	13.28
Saturated	y = -0.2823x + 13.13	-15.76	13.13
Dry	y = -0.114x + 6.33	-6.50	6.33

Table 6: Cohesion and friction angle of 80S/20K mixture

Batch	**Equation of trendline**	**Friction angle (degrees)**	**Cohesion (-)**
FT	y = -0.3432x + 13.83	-18	13.83
Saturated	y= 0.0609x + 2.22	3.49	2.22
Dry	y= 0.0531x + 3.73	3.04	3.73